TOPICAL REVIEW • OPEN ACCESS

Advancements in modelling human blood brain-barrier on a chip

Biofabrication

TOPICAL REVIEW

Advancements in modelling human blood brain-barrier on a chip

Vita Guarino[1,2,*], Alessandra Zizzari[2], Monica Bianco[2], Giuseppe Gigli[1,2], Lorenzo Moroni[2,3] and Valentina Arima[2]

[1] Department of Mathematics and Physics 'E. De Giorgi', Università del Salento, 73100 Lecce, Italy
[2] CNR NANOTEC—Institute of Nanotechnology, 73100 Lecce, Italy
[3] Department of complex tissue regeneration, Maastricht University, MERLN Institute for Technology-Inspired Regenerative Medicine, 6229ER Maastricht, The Netherlands
* Author to whom any correspondence should be addressed.

E-mail: vita.guarino@unisalento.it

Keywords: blood brain barrier, organ-on-chip, *in vitro* models, microfluidics

OPEN ACCESS

RECEIVED
23 September 2022

REVISED
9 December 2022

ACCEPTED FOR PUBLICATION
23 January 2023

PUBLISHED
14 February 2023

Abstract

The human Blood Brain Barrier (hBBB) is a complex cellular architecture separating the blood from the brain parenchyma. Its integrity and perfect functionality are essential for preventing neurotoxic plasma components and pathogens enter the brain. Although vital for preserving the correct brain activity, the low permeability of hBBB represents a huge impediment to treat mental and neurological disorders or to address brain tumors. Indeed, the vast majority of potential drug treatments are unable to reach the brain crossing the hBBB. On the other hand, hBBB integrity can be damaged or its permeability increase as a result of infections or in presence of neurodegenerative diseases. Current *in vitro* systems and *in vivo* animal models used to study the molecular/drug transport mechanism through the hBBB have several intrinsic limitations that are difficult to overcome. In this scenario, Organ-on-Chip (OoC) models based on microfluidic technologies are considered promising innovative platforms that combine the handiness of an *in vitro* model with the complexity of a living organ, while reducing time and costs. In this review, we focus on recent advances in OoCs for developing hBBB models, with the aim of providing the reader with a critical overview of the main guidelines to design and manufacture a hBBB-on-chip, whose compartments need to mimic the 'blood side' and 'brain side' of the barrier, to choose the cells types that are both representative and convenient, and to adequately evaluate the barrier integrity, stability, and functionality.

1. The organ-on-chips landscape

A bit like an aquarium recreating the marine ecosystem, Organ-on-Chips (OoCs) replicate the microenvironment of living organs. OoCs are often considered the nascent technology that will be able to replace animal models, in compliance with the principles of the 3Rs (Replacement, Reduction, and Refinement) developed over 50 years ago to provide a framework for performing more humane animal research [1]. Although that goal is still far off, using an *in vitro* OoC might help to shorten the portion of a clinical trial that tests a wide range of drug doses on patients to pinpoint the dose of a drug that is both effective and safe. Indeed, any toxicity observed with *in vitro* models can prevent unsuitable drug candidates from entering the expensive phase of clinical trials to limit costs and unrealistic expectations. However, OoCs are not formally validated yet and their use in the context of regulatory submissions is rare because of the lack of qualified assays in Good Laboratory Practice compliance [2]. It is not enough that OoCs respond to drugs as human organs to validate them, because these tests do not capture the full complexity of organs function, and chips may not include some complex signals such as those from the endocrine and immune systems [3]. Nevertheless, many pharmaceutical companies and government regulators are interested in OoCs use and refinement for their potential to reduce R&D costs [4]. Furthermore, beyond illuminating differences between animal models and humans with important outcomes in drug screening, OoCs may also support studies of disease modelling and regenerative medicine with interesting perspectives in the precision medicine field. For all these applications, a key aspect is to mimic in OoCs models the fluidic transport of vascularized tissues thanks to microfluidic

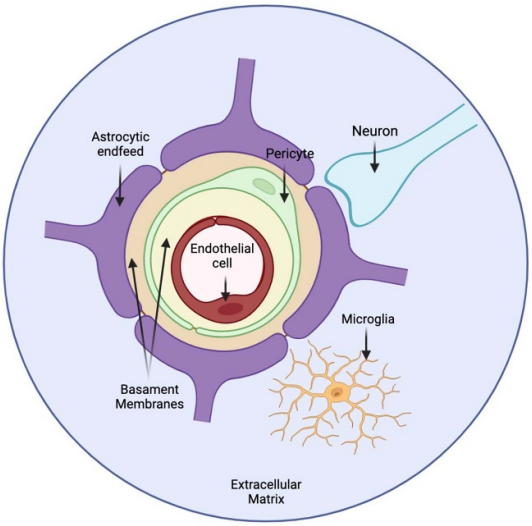

Figure 1. BBB structure: From the inside to the outside of the barrier, we find the capillary endothelial cells surrounded by pericytes, enclosed by the basement membranes, and the astrocytic endfeet covering the whole surface. The microglia and the synaptic terminals of neurons contact the barrier from the outside, where the extracellular matrix is located. Created with BioRender.com.

technologies. Particularly in the brain, vascularization has exceptional features, which are represented in the blood-brain barrier (BBB, figure 1). Using OoCs technology to develop a model of the human BBB (hBBB) is considered a promising way to overcome the limitations of rodent models and transwell systems, by combining the handiness of an *in vitro* model with the complexity of a living organ, while reducing costs and time [5].

In this review, we provide a critical overview of the biological and technological aspects of the OoC models for best recapitulating the hBBB features and functions. We classified the models developed so far into three main categories (also called layouts), described the main building blocks, cell types, and features, and analyzed the methods to assess barrier integrity. Finally, we concisely illustrated the applications of these models and some recent advances disclosing future perspectives in the medical field with strong impact on public health. Hence, far from being a comprehensive overview of disease modelling in hBBB-on-chips, the main purpose of this review is to describe the advancements in the development of hBBB *in vitro* OoC-based models and their technological challenges.

2. BBB models overview

Researchers wishing to study the complexity, functionality, and responsivity of BBB can apply two approaches: *in vivo* studies by animal models and *in vitro* studies by cell cultures. Recently, Jackson *et al* have extensively outlined *in vitro* and *in vivo* BBB model systems currently in use [6]. In this section, we provide a short overview of the gold standard models, which are rodent models (*in vivo*) and transwell systems (*in vitro*).

In vivo rodent models fulfill the requirements for the pharmacological evaluation of drug delivery across the BBB, considering the clinical need to determine the safety and efficacy of a new drug. However, the use of animal models is challenging, time-consuming, and costly because of many animals involved, animal-to-animal variability, and high doses of chemicals needed. There are also ethical issues concerning the use of animal models for clinical trials. Moreover, humans and rodents show insuperable structural differences such as genetic, immunologic, physiologic, and pathologic aspects that may influence the translation of preclinical results in clinical trials [6]. Indeed, more than 80% of potential therapeutics fail in human testing [7]. Nevertheless, rodent models are frequently used to investigate transport and metabolism in the context of the BBB thanks to the application of several methods such as intravenous injection, brain perfusion, positron emission tomography, and microdialysis sampling [8]. The two-photon imaging technique has even allowed studying both blood flow and the activity of individual cells below the surface of the brain in rats or mice [9].

In vitro transwell systems consist of more cell types cultured on semi-permeable microporous inserts in static wells, leading to compartmentalized co-cultures of the BBB cells derived by human tissues to achieve a multicellular human platform [10]. These models allow permeability or extravasation assays, and they are user-friendly, reproducible, and cost-effective, offering moderate scalability and high throughput screening [11]. However, transwell systems lack some key features of the BBB, such as the endothelium exposure to flow-induced shear stress (which plays a crucial role in modulating cell morphology, structure, and function) and the 3D microenvironment, acting as a functional scaffold pivotal for the cellular interactions and signals distribution [12, 13]. Moreover, in a transwell system, the 'edge effects' are not negligible since cells are unable to form a monolayer near the walls surrounding the membrane, resulting to be intrinsically very permeable [11].

Hence, both rodent models and transwell systems have several limitations that cannot be overcome even by combining both approaches together. In this scenario, the development of OoC models of the hBBB rises scientific challenges that are worth investigating.

3. hBBB features and functions

The hBBB is the boundary separating the blood from the brain parenchyma, controlling the exchange of substances, and the immune cells transport into the

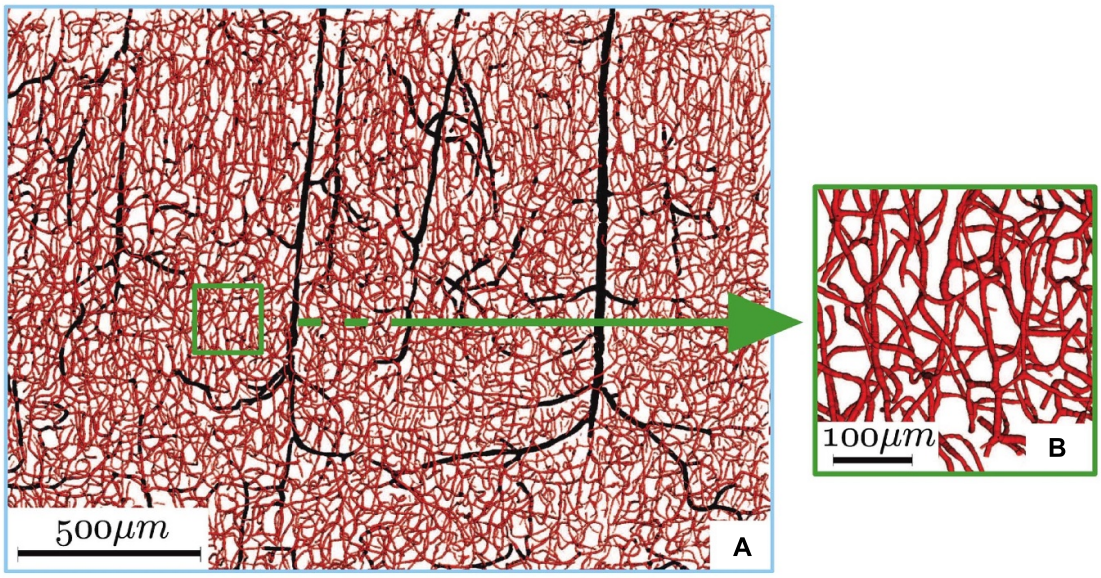

Figure 2. Human brain microvascular architecture: (A) in the brain intracortical region, the arteriolar and venular trees have a quasi-fractal structure (they are vessels of more than 10 μm in diameter, colored in black); (B) in contrast, the capillary bed is a dense mesh with vessels of less than 10 μm in diameter (colored in red). Adapted from [14] .

central nervous system (CNS), modulating the trafficking of pathogens. The hBBB consists of cellular (Endothelial Cells, Pericytes, Astrocytes, Microglia) and extracellular components, which are Extracellular Matrix (ECM) and Basement Membranes (BM). Interactions among these different cells and structures along with neurons refine a functional unit, called Neurovascular Unit (NVU), responsible for a dynamic system capable of regulating the local blood flow [15].

In this section, we report the main features and functions of the hBBB that must be considered to develop an OoC model. For that reason, here we first recall some fundamental notions related to the overall human brain microvascular architecture and then we briefly outline the contribution of each component of the hBBB. However, if the reader aims at raising its knowledge about the structure, function, and transport properties of the hBBB, we suggest reading the engineering perspective provided by Wong *et al* [16]. While to deepen the anatomy and immunology of vasculature in the CNS, we suggest reading the work of Mastorakos and McGavern [17].

3.1. Human brain microvascular architecture

The microvascularization of the human brain (figure 2) extends in length for about 600 km [18]. It is a multiscale network where, in contrast with the capillary bed, the arteriolar and venular trees have a quasi-fractal structure [14]. Individual capillary segments are between two junctions, and they are 7–10 μm in diameter with an average intercapillary distance of about 40 μm. Therefore, the cell body of a neuron is typically about 10–20 μm from the nearest capillary [16]. The region between capillaries and neurons is occupied by extracellular space, modelled as an interconnected network of 40–80 nm diameter tunnels, spanned by sheets between pairs of cell surfaces with a width of 10–40 nm [19].

Therefore, the development of an OoC modelling the hBBB starts from the level of complexity of the functional unit to replicate. Depending on the design strategies, as shown in section 4, the functional unit of a hBBB-on-chip model can be an individual capillary segment or a 3D network of capillaries.

3.2. Endothelial cells (ECs)

ECs line the brain microvessels lumen, connected by adherents junctions (AJs) and tight junctions (TJs). In particular, brain ECs are rich in TJs that play important roles in tissue integrity and vascular permeability. Indeed, they prevent the paracellular transport of most water-soluble compounds, including polar drugs, and severely restrict transport of small ions. Instead, the lipid membrane of the endothelium offers an effective diffusive route for lipid-soluble agents. TJs consist of transmembrane proteins, named claudin (CLDN) and occludin (OCLN), that link to the cytoskeleton through scaffolding proteins such as zonula occludens −1 (ZO-1), −2 (ZO-2), −3 (ZO-3), and cingulin [17]. Thus, transcellular transport is responsible for most molecular trafficking between the vascular system and the brain parenchyma [15]. Genes associated with junctional proteins and transporters of the ECs can be upregulated by shear stress associated with blood flow [12]. How brain ECs are affected by biomechanical inputs from the vascular system is an interesting matter

that merits further study. For instance, there are two works reporting *in vitro* effects of the flow on the endothelium morphology, both observed no elongation and alignment of brain ECs under flow [12, 20]. Especially, Ye's hypothesis was that ECs in the brain are programmed to resist elongation in response to curvature and shear stress, minimizing the length of tight junctions per unit length of capillary and hence minimizing paracellular transport into the brain [20]. Indeed, while there are many cells around the perimeter of large vessels, in small capillaries ECs can wrap around to form tight junctions with themselves, as well as their neighbors [21]. Nevertheless, Moya *et al* have recently observed ECs alignment in the direction of flow as well as significant morphological differences compared to static conditions in their OoC model of the hBBB, suggesting that brain microvascular ECs reorganize under flow conditions [22]. There are differences in the experimental setup that may explain these differing observations, as well the different cells type used: DeStefano used human brain microvascular ECs differentiated from human induced pluripotent cells (hiPSCs) line [12]; Ye used primary ECs from the brain microvasculature [20]; Moya used immortalized ECs from the brain microvasculature [22].

There is no doubt that the correlation between endothelial morphology and shear stress still needs exploration. OoC models of hBBB allow investigating this controversial issue better than traditional *in vitro* systems that do not include flow-induced shear stress.

3.3. Pericytes

Pericytes are the closest cellular connections with the endothelium, wrapping around precapillary arterioles, capillaries and postcapillary venules in the brain. In the human brain, the average ratio of pericytes to ECs is the highest (1:3–4). Pericytes have a prominent round nucleus that clearly differs from the elongated cigar-shaped nucleus of the ECs. The pericytes extend long processes that wrap the vessel wall with heterogeneous patterns, as a result of their functional differentiation [23]. A thin layer of the basement membrane, deposited by pericytes during development and angiogenesis, separates pericytes from ECs, and from surrounding astrocyte endfeet [24]. Although pericytes are usually quiescent, providing vascular stability, in the condition of a brain injury, they undergo phenotypic and functional changes that may include migration, proliferation or differentiation [25]. Indeed, pericytes have stem cell-like characteristics and can be differentiated into cell types from different lineages. Dore-Duffy *et al* reported that pericytes from cultured rat capillaries can also generate neurospheres with formation and differentiation rates higher in capillary cultures than in primary pericyte cultures [26]. Moreover, pericytes are contractile, with actin stress fibres throughout the cell body, and contribute to the regulation of cerebral blood flow by controlling capillary diameter [27]. Indeed, Kisler *et al* reported that a rapid progressive loss of pericyte coverage of cortical capillaries up to 50% in mice is correlated with approximately 50% reductions in stimulus-induced cerebral blood flow responses, with potential implications in neurological conditions [28]. Jamieson and co-workers studied the pericytes' contribution to the barrier function of an endothelial monolayer with different *in vitro* models. They compared the traditional transwell system to a microfluidic system, also applying physiological shear stress in the engineered microvessel with a cylindrical geometry. In both systems, the presence of pericytes had no effect on the barrier function of a healthy endothelial monolayer [29]. The most supported hypothesis is that an optimal endothelial monolayer does not require other cell types to ensure physiological barrier function, while a stressed one can be partially or fully rescued through the secretion of soluble factors from other cell types.

Simulating stress or damages in OoC models of the hBBB can help to further explore the pericytes' role, because they can recapitulate the correct spatial arrangement with pericytes at the interface between the endothelium of microvessels and the surrounding matrix. The pericytes' motility and distribution towards microvessels of OoC models may be a charming subject of study, for instance.

3.4. Astrocytes

Astrocytes, which are specialized glial cells, make synapses between neurons and contacts with brain microvessels thanks to their cellular processes named 'astrocytic endfeet', which form a continuous sheath covering the microvessels. The thickness of this glial sheath varies from 300 nm down to 20 nm, with endfoot–endfoot clefts of 20 nm width [30]. Astrocytic endfeet show several specialized features of this location, including a high density of the water channel aquaporin 4 (AQP4) and the Kir4.1 K+ channel, which are involved in ion and volume regulation [15, 17]. Furthermore, AQP4 has a crucial role in the 'glymphatic pathway' proposed by Iliff *et al* to explain the mechanism of ECM debris removal through NVU and cerebrospinal fluid (CSF) active directional filtration [31, 32]. There are many different astrocytic factors that regulate barrier permeability, with a key role in BBB recovery after brain damage [33]. Some more well-known astrocytic factors are glutamate, aspartate, interleukin-1β (IL-1β), endothelin-1, nitric oxide, interferon-γ, and tumor necrosis factor-α (TNFα) [17]. The appropriate control of these factors may be significant to protect against brain injury induced by BBB disruption.

The clinical use of an astrocyte-targeted therapy is a promising approach that encourages further investigation of astrocytic functions. It is with this in mind that OoC models of the hBBB may allow studying

in vitro the selective and controlled modulation of astrocytes while interacting with the other cells of the BBB in physio/pathological conditions.

3.5. Microglia

Microglia are the first cellular lines in the innate immune response of CNS, acting as specialized resident macrophage, which can mediate the loosening of BBB and the secondary immune reaction [13]. In the healthy brain, microglia bodies are relatively immobile, but they extrude numerous protrusions with secondary branches used for the continuous exploration of the microenvironment. Under pathological conditions, microglia cells are activated in order to play a pro-inflammatory function or on the contrary a pro-angiogenic and immunosuppressive role. Activated microglia can be recognized by a deramified phenotype with retracted and thicker processes and enlarged cell bodies [34]. BBB-associated microglia preferentially localize along the vasculature in locations where astrocytic endfeet coverage is absent [35]. Microglia exert dual detrimental and protective properties on the BBB. Based on the current knowledge, pro-inflammatory microglia (M1) contribute to BBB dysfunction and vascular 'leak', while anti-inflammatory microglia (M2) play a protective role in the BBB [36]. However, the role of microglia in regulation of the BBB phenotype still needs to be thoroughly investigated. The endothelial and non-endothelial components of the BBB can influence microglia via blood-derived factors, or endothelium-, pericyte- and ECM-derived mediators [37]. Increasing our knowledge of microglia–BBB interactions may disclose how BBB dysfunction and neuroinflammation are associated with CNS diseases.

Modulation of microglial activation by suppressing the deleterious effects and simultaneously retaining the protective functions on the BBB, could allow to develop novel therapeutic targets. OoC models of hBBB will aid in meeting this challenge because they allow advancing the study of cell–cell interactions at the BBB interface by the evaluation of microglial effects on barrier permeability and biomarker expression.

3.6. ECM and basement membranes (BM)

The ECM, surrounding the cells in the brain parenchyma, is mainly composed of proteoglycans, hyaluronan, link proteins and tenascins [38]. The cellular components of BBB and ECM are functionally and structurally integrated, controlling the bidirectional exchange of nutrients, cytokines, molecular mediators, and immune cells between CNS and systemic circulation [13]. The Basement Membranes (BMs) are a unique form of the ECM, with many functions, including structural support, cell anchoring and signalling transduction. Structurally, the BMs are highly organised protein sheets with thicknesses of 50–100 nm. Biochemically, the BMs consist of four major ECM proteins: collagen IV, laminin, nidogen and perlecan (also known as heparan sulfate proteoglycan 2, HSPG2) [39].

In the brain, two types of BMs are found: endothelial BM (inner) and parenchymal BM (outer), which enclose pericytes. In capillaries, the outer BM is adjacent to the inner BM, whereas the postcapillary venules are surrounded by a perivascular CSF-filled space that separates the inner BM from the outer BM. These spaces support a lot of immune activity, playing a major role in compartmentalizing CNS immune reactions [17]. During a diseased state of the CNS, the ECM undergo profound changes including the remodelling and enzymatic degradation of ECM proteins. ECM remodelling can lead to BBB disruption or contribute to BBB repair according to the biphasic ECM regulation following vascular damage [40]. Among the extracellular proteases of the CNS involved in the ECM turnover, there are more than 20 members of matrix metalloproteinases (MMPs). However, our knowledge of the molecular mechanisms underlying ECM remodelling and turnover in CNS diseases is still limited.

ECM-targeted therapy could become promising for the treatment of CNS diseases if biomarkers to monitor ECM remodelling will be identified. Therefore, simulating the BBB breakdown in OoC models may aid to detect ECM molecules and extracellular proteases able to pass directly into the vascular system by studying mechanism and timing. Consequently, a careful ECM composition in a OoC model of hBBB appears crucial.

4. Development of hBBB-on-chip models

In this section, we deepen the design strategies to develop hBBB-on-chip models. The design of a hBBB-on-chip model must consider two main areas: the 'blood side', mimicking the microvascular lumen of the brain capillary bed; and the 'brain side', mimicking the abluminal side of the capillaries and the brain parenchyma. Based on the spatial arrangement of the blood side and the brain side in the device, three main layouts can be defined: (i) side-by-side layout, where the blood side and the brain side are on the same plane (figure 3(A)); (ii) double-layer layout, where the brain side and the blood side are on two overlapped planes (figure 3(B)); (iii) hollow channel layout, where the blood side is surrounded by the brain side (figure 3(C)).

Regardless of the layout, we can identify three main elements that are common to all the models: building blocks to device manufacture, cell types to be included, and hBBB features to reproduce. Thus, we collected and examined published works developing microfluidic models of BBB made strictly of human cells (table 1), exempting those including merely brain ECs without any cellular component

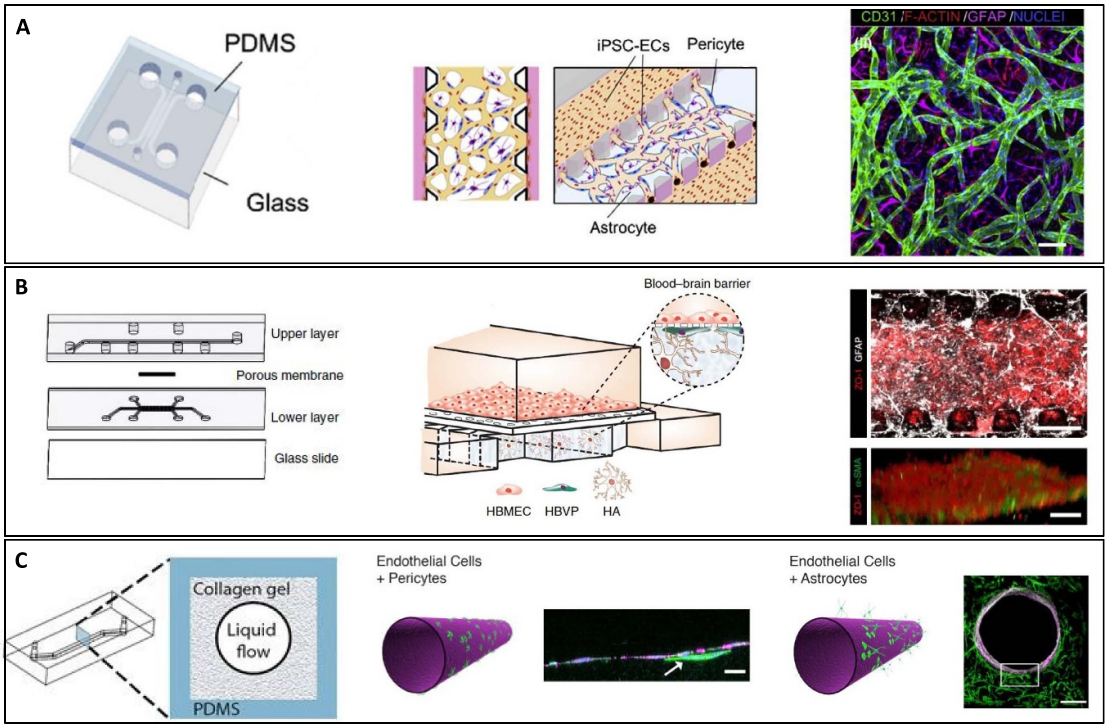

Figure 3. Examples of hBBB-on-chip models with different layouts. (A) Side-by-side layout. Adapted from [50], Copyright (2018), with permission from Elsevier. (B) Double-layer layout. Adapted from [49], with permission from Springer Nature. CC BY 4.0. (C) Hollow channel layout. Adapted from [53]. CC BY 4.0.

of the brain side. Being mainly focused on biological and technological aspects, we avoided describing the recent, although valuable in the medical field, advances of devices already reported. Rather, if the reader is interested to further the applications of OoC models of hBBB to the clinical field, such as disease modelling and drug testing, we suggest the recent work of Cui and Cho [41].

4.1. Building blocks

The building blocks to manufacture a hBBB-on-chip model are (a) chip, (b) hydrogel, and (c) membrane (or fibre).

Chips with microfluidic patterns are commonly fabricated by photolithography and soft lithography. Indeed, most of the reported hBBB-on-chip models are fabricated by standard polydimethylsiloxane (PDMS) replica molding. Briefly, the microfluidic chip is made by casting PDMS prepolymer and curing agent at a weight ratio of 10:1 onto a patterned SU-8 master. The polymer is cured in an oven and subsequently peeled off from the mold. Additionally, cutting-edge technologies such as 3D printing and two-photons lithography were successfully used to produce microfluidic chips as BBB models, but they did not describe a human model [42, 43]. Moreover, the 3D bio-printing methods showed a promising application for the OoCs fabrication, even if a hBBB model did not come out yet [44]. Indeed, it is worth mentioning Kolesky's work developing a method enabling cell-laden hydrogel to be poured around a printed sacrificial element, which is subsequently flushed away to leave the channel free for endothelial cell seeding and perfusion through the connection to a microfluidic pump [45]. Furthermore, in the recent work of Dobos *et al*, the two-photon polymerization allowed to print directly on a chip microvascular structures (10–30 μm in diameter) [46].

Hydrogels are essential for assembling a 3D cell culture inside a microfluidic device. For instance, hydrogel filling the brain side of hBBB-on-chip models with a double-layer layout allowed to have a 3D cellular microenvironment like *in vivo* brain parenchyma [47–49]. Meanwhile, in some models with a side-by-side layout, the hydrogel was exploited to obtain a 3D self-organized microvascular network by angiogenic or vasculogenic processes [50–52]. Hydrogels were also used to fabricate a cylindrical channel inside a microfluidic device to build hBBB-on-chip models with a hollow channel layout. For instance, thanks to the viscous fingering technique, Herland *et al* developed a lumen in a collagen gel where astrocytes were incorporated (the brain side), while ECs and pericytes lined the lumen of the channel (the blood side) [53]. Alternatively, a hydrogel gelled around a needle into the housing device allowed to have a hollow channel layout [54]. Finally, the development of novel photo-curable hydrogels is crucial to fabricate

Table 1. Summary of current hBBB-on-chip models.

		Building blocks			Features of 'blood side'		Features of 'brain side'		Type of cells	Type of analysis		
Layout	References	Chip	Hydrogel	Membrane (or Fibre)	Approach, Shape and Size	Culture conditions and Shear stress	ECM materials	Cells distribution	Primary/ Immortalized/ hiPSCs	TJs	Permeability	TEER
Double-layer	[47]	Photolithography and soft lithography/ PDMS	Acting as ECM	Polycarbonate membrane: 0.2 μm pore size	Templating: rectangular chamber (base 3 mm × 6.2 mm, height 100 μm)	Dynamic: syringe or peristaltic pump, flow rate of 2 μl min^{-1} (shear stress n.a.)	Collagen type I	2D co-culture of PCs and ACs. Neurons embedded in 3D matrix.	Primary: hBMVECs, PCs, and ACs. hiPSC-derived: Neurons.	ZO-1	10 kDa or 70 kDa FITC-Dextran, Ascorbate	Measuring impedance (range of frequencies)
	[56]	Photolithography and soft lithography/ PDMS	—	Polyethylene terephthalate membrane: 0.4 μm pore size	Templating: straight rectangular channel: height 0.2 mm, width 1 mm	Dynamic: peristaltic pump, flow of 1 μL min^{-1}, shear stress of 0.02 dyne/cm^2	—	2D co-culture of PCs and ACs.	Primary: hBMVECs, PCs, and ACs	ZO-1	530 Da Cascade Blue, 67 kDa BSA-555	n.a.
	[48]	Photolithography and soft lithography/ PDMS	Acting as ECM	Polyethylene terephthalate membrane: 8 μm pore size	Templating: straight rectangular channel (height 200 μm, width 800 μm)	Static, convertible in dynamic by syringe pump (flow rate and shear stress n.a.)	Collagen type I, Matrigel, Glycosil hyaluronic acid	ACs embedded in 3D matrix.	hiPSC-derived: ECs and ACs.	ZO-1, occludin, claudin-5	Sodium fluorescein	Measuring impedance (range of frequencies)
	[57]	Photolithography and soft lithography/ PDMS	—	PDMS membrane: 7 μm pore size	Templating: straight rectangular channel (height 100 μm, width 200 μm)	Dynamic: peristaltic pump, flow rate of 30, 1500, or 6500 μl h^{-1}, equivalent shear stress of 0.01,0.5, or 2.4 dyne/cm^2	—	2D co-culture of PCs and ACs. Or, 2D hiPSC-derived neural cultures	Primary: PCs and ACs. hiPSC-derived: ECs, Neural cells.	ZO-1, occludin, claudin-5	3 kDa FITC-Dextran	Measuring impedance (range of frequencies)
	[49]	Photolithography and soft lithography/ PDMS	Acting as ECM	Polycarbonate membrane: 8 μm pore size	Templating: straight rectangular channel(height 100 μm, width 400 μm)	Dynamic: syringe pump, flow rate of 16 μl min^{-1}, shear stress of 4 dyne/cm^2	Matrigel	2D culture of PCs. ACs embedded in 3D matrix.	Primary: PCs and ACs. Immortalized: HBMEC.	ZO-1	4 kDa or 40 kDa FITC-Dextran	measuring ohmic resistance (single frequency of 12.5 Hz)

(Continued.)

Table 1. (Continued.)

		Building blocks			Features of 'blood side'		Features of 'brain side'		Type of cells	Type of analysis		
Layout	References	Chip	Hydrogel	Membrane (or Fibre)	Approach, Shape and Size	Culture conditions and Shear stress	ECM materials	Cells distribution	Primary/ Immortalized/ hiPSCs	TJs	Permeability	TEER
	[58]	Photolithography and soft lithography/ PDMS	—	PDMS membrane: 5 μm pore size	Templating: straight rectangular channel (height 50 μm, width 500 μm)	Static: gravity-driven flow by inserting medium filled pipette tips in the access ports of device	—	2D culture of ACs.	Primary: ACs. Immortalized:HCMEC/D3.	ZO-1	4 kDa or 20 kDa FITC-Dextran	n.a.
Side-by-side	[59]	Photolithography and soft lithography/ PDMS	Acting as ECM	Chitosan membrane (temporary)	Templating: straight channel (height n.a., width n.a.)	Static: hydrostatic pressure was applied to the cells by placing pipette tips with unequal medium amounts on the inlets and outlets	Matrigel	ACs embedded in 3D matrix.	Primary: ACs. Immortalized:HCMEC/D3.	n.a.	n.a.	n.a.
	[60]	Photolithography and soft lithography/ PDMS	—	Hollow Fibre in Alginate: 400 μm inner diameter, 500 μm outer diameter	Templating: straight rectangular channel housing the hollow fibre externally lined by ECs	Static	—	2D culture of ACs.	Primary: ACs and HUVECs.	n.a.	40 kDa FITC-Dextran	n.a.
	[51]	Photolithography and soft lithography/ PDMS	Supporting the formation of interpenetrating vascular and neuronal networks	—	Self-organizing: vascular lumens with an average diameter of $\sim$ 60 μm	Static: hydrostatic pressure was applied thanks to large medium reservoirs connected to the microfluidic devices	Porcine skin collagen	3D co-culture of ECs and motor neuron spheroids (diameter $<$150 μm).	Human ES-derived neuronal stem cells (hNSC). hiPSC-derived: ECs.	n.a.	40 kDa FITC-Dextran	n.a.

(Continued.)

Table 1. (Continued.)

		Building blocks			Features of 'blood side'		Features of 'brain side'		Type of cells	Type of analysis		
Layout	References	Chip	Hydrogel	Membrane (or Fibre)	Approach, Shape and Size	Culture conditions and Shear stress	ECM materials	Cells distribution	Primary/ Immortalized/ hiPSCs	TJs	Permeability	TEER
	[50]	Photolithography and soft lithography/ PDMS	Supporting vasculo-genesis	—	Self-organizing: vascular lumens with nearly circular cross-section an average lateral diameter of 42 ± 13 μm, an average transverse diameter of 25 ± 6 μm)	Static	Fibrin	3D triple co-culture of ACs, PCs and ECs.	Primary: PCs and ACs. hiPSC-derived: ECs.	ZO-1, occludin, claudin-5	10 or 40 kDa FITC-dextran	n.a.
	[61]	Photolithography and soft lithography/ PDMS	Separating brain side from the blood side	—	Templating: straight rectangular channel (height 220 μm, width 400 μm)	Dynamic: continuous perfusion generated by placing the device on a rocker platform, creating a bidirectional flow, with a shear stress of 1.2 dyne/cm^2	Collagen type I	2D co-culture of ACs and PCs.	Immortalized: ECs, ACs, and PCs.	Claudin-5	20 kDa FITC-dextran	n.a.
	[52]	photolithography and soft lithography/ PDMS	Supporting vasculo-genesis	—	Self-organizing: vascular lumens with an average diameter of 34.64 μm	Static	Fibrin	3D triple co-culture of ACs, PCs and ECs.	Primary: hBMVECs, PCs (from placenta), and ACs.	ZO-1, occludin, claudin-5	10 kDa or 70 kDa FITC-dextran	n.a.
	[62]	Photolithography and soft lithography/ PDMS	—	—	Templating: circular rectangular channel (height 100 μm, width 200 μm)	Dynamic (after 3 d under static conditions): syringe pump, flow rate from 100 nL min^{-1}–5 μl min^{-1}, shear stress from 0.05 dyne cm^{-2}–2.73 dyne/cm^2	—	2D culture of ACs.	Primary: ACs. Immortal-ized:HCMEC/D3.	ZO-1, claudin-5	10 kDa or 70 kDa FITC-dextran	n.a.

(Continued.)

Table 1. (Continued.)

		Building blocks			Features of 'blood side'		Features of 'brain side'		Type of cells	Type of analysis		
Layout	References	Chip	Hydrogel	Membrane (or Fibre)	Approach, Shape and Size	Culture conditions and Shear stress	ECM materials	Cells distribution	Primary/ Immortalized/ hiPSCs	TJs	Permeability	TEER
Hollow channel	[53]	Photolithography and soft lithography/ PDMS	Forming a cyl-indrical wall and acting as ECM	—	Templating: straight cylindrical channel obtained by viscous fingering technique (∼600-800 μm lumen diameter, 2 cm long)	Static: hydrostatically driven flow of 120 μl min^{-1}, shear stress of ∼1 dyne/cm^2	Collagen type I	2D culture of PCs lining the cylindrical lumen. ACs embedded in 3D matrix of the cylindrical wall.	Primary: hBMVECs, PCs, and ACs.	ZO-1	3 kDa Alexa-488 dextran	n.a.
	[54]	Photolithography and soft lithography/ PDMS	Forming a cyl-indrical wall and acting as ECM	—	Templating: straight cylindrical channel obtained by a 180 μm-diameter acupuncture needle inserted into the needle guides of the device	Dynamic: 2.4 μl min^{-1} volumetric flow rate, to exert approximately 0.7 dyne cm^{-2} of shear stress on the endothelium within the channel. Applied also a cyclic and pulsatile flow	Matrigel, Thiol-modified hyaluronan, and Collagen type I	ACs embedded in 3D matrix of the cylindrical wall	Primary: ACs. Immortal-ized:HCMEC/D3.	ZO-1	4 kDa FITC-dextra	Measuring impedance (range of frequen-cies)
	[22]	Photolithography and soft lithography/ PDMS	Filling a cyl-indrical abluminal space and acting as ECM	Hollow Fibre in PVDF: 0.65 mm inner diameter, 1.2 mm outer diameter, 0.2 μm pore size (swollen state)	Templating: multiple straight rectangular channels housing the hollow fibres internally lined by ECs (luminal space)	Dynamic: peristaltic pump, flow rate of 0, 94.7, 380, and 2100 μl min^{-1}, corresponding to shear stresses of 0.77, 3, and 17 dyne/cm^2	Collagen and fibronectin	ACs embedded in 3D matrix	Primary: ACs. Immortal-ized:HCMEC/D3.	ZO-1	4, 20, 120 kDa FITC- or TRITC-dextran	n.a.

'bio-printed' OoCs, as previously mentioned. Indeed, several approaches have been developed to introduce reactive groups to the biopolymers allowing the photopolymerization [55].

Membranes (or alternatively fibres) are key elements to partition the compartments of a microfluidic device while providing structural support for cell layers, and preserving physical and biochemical cross-talk between cells. Most hBBB-on-chip models with a double-layer layout use a commercial membrane made in Polycarbonate (PC) or Polyethylene terephthalate (PET) [47–49, 56], integrated by functionalization with 3-aminopropyltriethoxysilane (APTES) according to what reported from Aran and colleagues [63]. However, some researchers preferred a porous membrane in PDMS for its high transparency compared to the other membranes, which allows non-invasive monitoring of cells during cell culture without resorting to labeling [57, 58]. Instead, Tibbe *et al* developed a temporary membrane separating channels in a model with a side-by-side layout to allow the seeding of cells separately in each channel and to put them in direct contact after membrane deletion [59]. A similar strategy could be developed and applied to the other layouts, opening a new class of OoCs in which cells are not separated by artificial barriers and interact with each other more strictly as *in vivo*. For example, recently, Arik *et al* have proposed a collagen-based enzymatically degradable membranes for OoC barrier models [64]. Indeed, collagen is an actual part of the *in vivo* ECM, and collagen-based membranes can be treated with proteases to modulate fibre thickness and permeability. Their results provide a preliminary study to develop more representative models and deepen the disease-related ECM remodelling. A further interesting approach was used by Huang *et al*, which developed a few hundred nanometers thick monolayer of nanofibres by electrospinning of a gelatin solution. They used electrospun nanofibres as an artificial physiologically relevant basement membrane to separate two compartments in a device with a double-layer layout [65]. Although both Arik's and Huang's devices are not applied to model the hBBB, it is easy to imagine it for future developments. Indeed, an approach similar to Huang's chip has been already demonstrated in a transwell-like hBBB model, consisting of a 3D printed holder and an electrospun poly(lactic-co-glycolic acid) (PLGA) mesh as an insert [66]. Finally, some hBBB-on-chip models have a hollow fibre in place of a separating membrane. For instance, Nguyen *et al* developed their hollow fibre in alginate covered by ECs on the abluminal side and placed in the channel of a microfluidic device with a side-by-side layout [60]. Instead, Moya *et al* used a commercial hollow fibre in polyvinylidene fluoride (PVDF), enclosed in a microfluidic device to obtain a hollow channel layout [22].

4.2. Type of cells

The cellular players of a hBBB-on-chip model are basically the ECs into the blood side, while pericytes and astrocytes into the brain side. However, even neurons and microglia could be included in the brain side with the aim of replicating the NVU.

ECs are the most important cells in the hBBB, and the use of the primary human brain microvascular endothelial cells (hBMVECs) should be the best choice pursuing the development of a human model, including the primary human brain pericytes (PCs) and astrocytes (Acs). However, the isolation of primary hBMVECs has a high workload, they are very expensive and require time to reach confluence [67]. Originally, many works on hBBB models reported the use of human umbilical endothelial cells (HUVECs), but these cells are a model of large vessels and do not exhibit the required barrier properties and functions. A good alternative is represented by the immortalized human cerebral microvascular endothelial cell line HCMEC/D3, developed by Weksler *et al*, showing fundamental properties of primary human BMECs, including tight junction/transporter protein expression and contact growth inhibition, for up to 35 passages [68].

Additionally, the recent development of human-induced pluripotent stem cells (hiPSCs) technology is fascinating for those who wish to study the hBBB role in nervous system diseases. Since hiPSCs can be derived from patients, researchers may simultaneously generate multiple cell types and study neurological disorders within an endogenous human model. Unluckily, working with hiPSCs has some disadvantages as batch-to-batch variability and high costs, and it is technically challenging and time-consuming [69]. To date, there is not a fully isogenic hBBB-on-chip model that means the complete incorporation of all hiPSCs-derived components of the hBBB [47, 48, 50, 51, 57]. However, it is worth mentioning that the model developed by Vatine and co-workers incorporating hiPSCs-derived ECs of Huntington's disease (HD) patients, co-cultured with primary brain vascular pericytes and astrocytes, showed an increasing barrier permeability than the same model with healthy control hiPSCs [57].

4.3. Features of the 'blood side' and 'brain side'

With the aim to replicate in a OoC model the features of the two different sides (blood and brain) of the hBBB, researchers must keep in mind (a) the microvessels *in vivo* architecture and size to design the chip geometry of the blood side; (b) effects of cell exposure to the flow-induced shear stress during pumping through the blood side; and, (c) the 3D microenvironment and ECM composition of the brain side.

The shape and size of the blood side in a hBBB-on-chip model impact the endothelium properties,

such as cell distribution, orientation, and alignment. The most reported shape of the blood side is a single straight rectangular channel, with a minimum aspect ratio of 2:1 related to a width of 200 μm and a height of 100 μm [47, 57]. In such a case, we refer to a 'templating' approach for modelling a microvessel on a chip by cells lining the microchannel walls and forming an endothelial monolayer with a predetermined architecture and well-defined size. This approach is the most used being effective and reliable, although the human brain capillaries appear as complex arrays of tubular vessels with a critical average diameter of 10 μm [16]. Indeed, realizing networks of tens of microns in size is challenging due to limitations of the templating fabrication methods, or difficulties in delivering fluids through small artificial capillaries. Contrariwise, a 'self-organizing' approach is based on filling the chip with a 3D matrix and promoting an angiogenic or vasculogenic process to obtain *ex-novo* microvessels, well-connected and perfusable, with shape and size more like a 3D physiological network. Although quite bio-mimicking, this approach lacks reproducibility since it does not guarantee full control of the intraluminal flow because of the spontaneous forming of an unpredictable and complex architecture. To date, the average diameter of 34.64 μm reported by Lee *et al* is the smallest engineered vessel diameter reached in a hBBB-on-chip by using the self-organizing approach [52]. Therefore, all current hBBB-on-chip models are still far off from reaching the human brain capillaries dimensions.

With respect to the cell exposure to the flow-induced shear stress in the blood side of a hBBB-on-chip model, getting a dynamic cell culture on a chip is the keystone. Indeed, reproducing physiological shear stresses is crucial to effectively model the ECs arrangement and integrity of the hBBB. Initially, several hBBB-on-chip models allowed only static cell cultures, easy to accomplish by connecting the microchannels to some media feed reservoirs and merely refreshing the medium [50, 52, 60]. Then, some microfluidic systems were improved by applying hydrostatic pressure to the microchannels, for instance, by placing pipette tips with unequal medium amounts at the inlets and outlets [48, 51, 58, 59]. However, the intraluminal flow generated by hydrostatic pressure is low compared to the flow-induced shear stress experienced by brain microvessels. Indeed, the flow rate in brain capillaries typically ranges from 6 to 12 nl min^{-1} corresponding to a shear stress of 10–20 dyne cm^{-2} for a capillary of 10 μm in diameter [16]. Instead, a lower shear stress of 1–4 dyne cm^{-2} is representative of the brain venous system [12]. Therefore, a dynamic culture by a peristaltic or a syringe pump to generate continuous cell exposure to the flow is needed to get realistic shear stresses in hBBB-on-chip models [22, 49, 57]. Although multi-pumping systems are suitable to study more devices at the same time, the long multiple tubes that connect the devices located in a CO_2-incubator to pumps (outside the incubator) could be an obstacle in many steps of the culture and may increase the probability of air bubbles generation. Moreover, for some microfluidic devices, it would be exorbitantly expensive to run a cell culture under continuous flow for many days to get realistic shear stresses, as it may happen for the model developed by Herland *et al* where they would need flow rates in the range of 600 ml h^{-1} [53]. Another strategy of microchannels perfusion is using a rocker platform, allowing the medium to flow from inlet to outlet and back, creating a bidirectional flow, regulating the inclination angle, and the interval with which the rocker platform switches sides [61]. Despite some efforts, the research of a hBBB-on-chip model able to incorporate physiological shear stresses is still challenging, and it is a key aspect to effectively reproduce the ECs arrangement and the barrier integrity.

Finally, we need to consider the features of a hydrogel filling the brain side of a hBBB-on-chip model to replicate the 3D brain microenvironment (cell-cell and cell-ECM interactions) and allow more realistic cellular responses. The most used hydrogels in hBBB-on-chip models as 3D matrices are made in naturally-derived materials: Matrigel [49, 59], collagen [47, 51, 53], and fibrin [50, 52]. Indeed, these hydrogels mimic salient elements of native ECM, have mechanical properties near to those of many soft tissues (e.g. brain parenchyma), support cell adhesion, and regulate cell behavior. Moreover, their structure undergoes remodelling by the cultured cells, like *in vivo*, thanks to the degradation and deposition of ECM proteins. At the same time, naturally-derived hydrogels meet some significant technical requirements, such as suitable optical properties to allow visualization of cells *in situ* by imaging, or a good chemical degradability to recover alive cells from the matrix for molecular and cellular analyses. Despite their advantages, these hydrogels have some common drawbacks such as low stiffness, limited long-term stability, and batch-to-batch variability [70]. Although there are other hydrogel options (e.g. synthetic or hybrid materials) that can be explored to have more well-defined and tunable platforms, naturally-derived hydrogels are the most used by researchers to develop OoC models.

5. Barrier assessment of hBBB-on-chip models

The BBB integrity of a model can be assessed by qualitative and quantitative methods, allowing for the comparison of *in vitro* model outcomes with those *in vivo*. The most common methods are tight junctions (TJs) immunolabeling, permeability assays, and TEER reading.

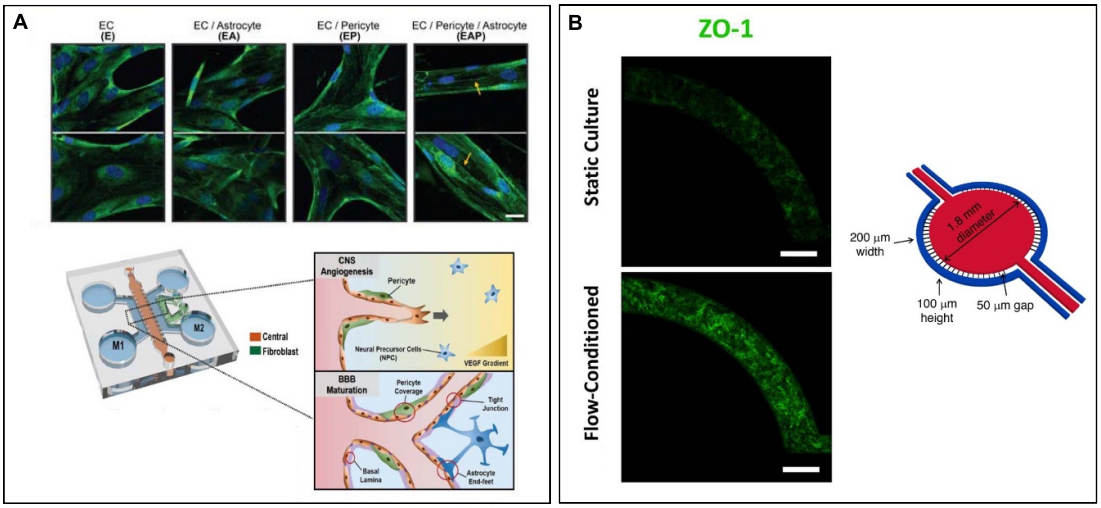

Figure 4. ZO-1 visualization in two different hBBB-on-chip models. (A) 3D model based on a side-by-side layout chip and a self-organizing approach. Adapted from [52] John Wiley & Sons. © 2019 Wiley Periodicals, Inc. (B) 2D model based on a side-by-side layout chip and a templating approach. Adapted from [62] John Wiley & Sons. © 2018 The Authors. Bioengineering & Translational Medicine published by Wiley Periodicals, Inc. on behalf of The American Institute of Chemical Engineers. CC BY 4.0.

TJs immunolabeling is used to preliminary evaluate the barrier integrity. The immunostaining of proteins characteristic of tight junctions found *in vivo* (ZO-1, Occludin, and Claudin-5) provides qualitative insights into the endothelial monolayer *in vitro*, by imaging with fluorescent microscopy [71]. The barrier integrity is further assessed by measuring the flux of tracer molecules (often fluorescently labeled) across the endothelium and quantified by the endothelial permeability coefficient (named apparent permeability, P_{app}). The permeability of BBB is affected by the paracellular water flow, as well as the pore size of the tight junctions [72]. *In vivo*, BBB permeability of microvessels in the rat brain tissue was assessed by the cerebral circulation of FITC-dextran −4 kDa, −20 kDa, −40 kDa, −70 kDa, resulting to be 6.2, 1.8, 1.4, 1.3×10^{-7} cm s^{-1}, respectively [73]. Finally, TEER measures the ion flux through the barrier. It gives an indication of the tightness of cell–cell junctions in the paracellular space of cellular monolayer by means of electrical resistance readings. *In vivo* TEER values measured in rat brain surface microvessels have been reported to be 800 Ω cm^2 as the average resistance of venous microvessels, and 2000 Ω cm^2 as the average resistance of arterial microvessels, with an overall average of 1500 Ω cm^2 that is considered the reference value for *in vitro* BBB models [74, 75]. However, these TEER values were unlike those previously reported by Smith *et al* that calculated an electrical resistance of 8000 Ω cm^2 for brain parenchymal vessels in adult rats from the combined permeability of radioisotopic sodium, potassium, and chloride [76].

For the evaluation of the barrier integrity of a hBBB-on-chip model, researchers should optimize specific protocols to execute on a chip the immunolabeling of TJs proteins of the endothelium, permeability measurement, and TEER reading. Then, these methods can be used to investigate how a hBBB-on-chip model is affected by some stimuli like cellular exposure to different shear stresses or the delivery of drug formulations.

5.1. TJs immunolabeling

Among the TJs proteins of the endothelium, ZO-1 is the most considered marker for the endothelial tightness of a hBBB-on-chip model. The visualization of ZO-1 allows a quick qualitative comparison among different chips or different conditions of the same chip (figure 4). For instance, Lee and colleagues compared the confocal images of ZO-1 expression for each culture condition tested in their 3D hBBB-on-chip model (figure 4(A)): ECs, ECs/Astrocytes (EA), ECs/Pericytes (EP), or ECs/Pericytes/Astrocytes (EPA). They reported that ZO-1 expression in a monoculture of ECs was not significant around the cell-to-cell boundary, but rather distributed over the cell body. When ECs sprouted in the presence of astrocytes (condition EA), the boundaries between ECs were visible through the ZO-1 junction. However, the expression signal was weaker than that under conditions EP and EAP. Condition EAP exhibited the strongest ZO-1 intensity with a clear zipper-like boundary between ECs. These differences in fluorescence intensity meant that the expression of the ZO-1 tight junction proteins was determined by cellular interactions between ECs and surrounding BBB perivascular cells [52]. Instead, Brown and co-workers performed immunostaining for ZO-1 on their 2D hBBB-on-chip model after culturing 3 d

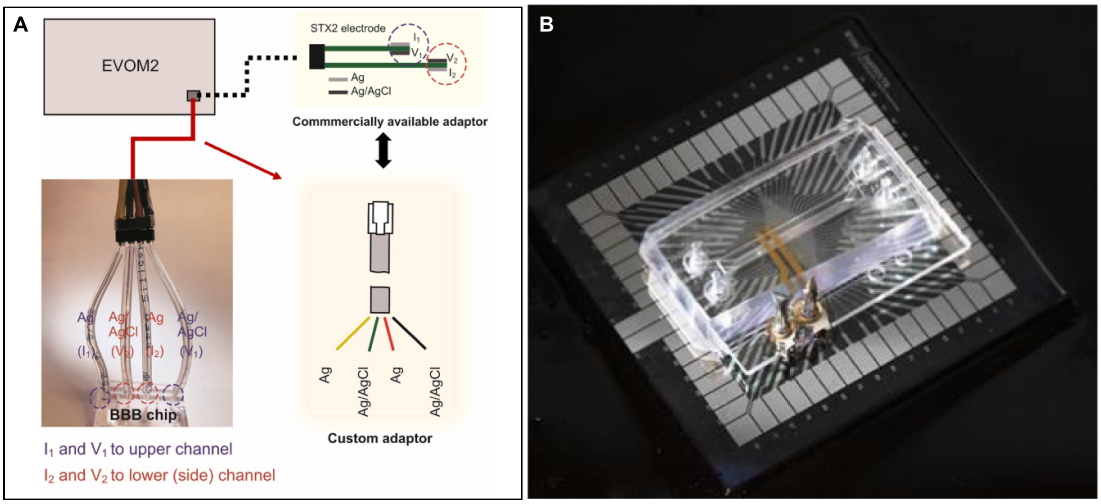

Figure 5. Examples of dedicated setup for the TEER reading on a chip. (A) Customized system based on two couples of Ag, AgCl wire electrodes to read the ohmic resistance by using a commercially available volt-ohmmeter (EVOM2). Adapted from [49], with permission from Springer Nature. CC BY 4.0. (B) Multi-Electrode Array (MEA) chip with connectors in Platinum (gray) and the TEER electrodes in gold. Reproduced from [77] with permission from the Royal Society of Chemistry.

statically and after conditioning to physiologically relevant fluid flow (figure 4(B)). The TJs expression profile increased dramatically in the flow-conditioned model, similar to the *in vivo* hBBB, as compared to its static counterpart [62].

5.2. Permeability assays

A real-time representation of the barrier integrity of hBBB-on-chip models can be obtained by methods that do not compromise cell viability, like the permeability measurement. Thus, a blank measurement of permeability (chip without cells) should be subtracted from the measured permeability of cells grown into the device to calculate the permeability coefficient (P_{app} index) of the endothelium *in vitro*, to be compared with the permeability recorded *in vivo*. Although, it must be considered that any tracer compounds may interfere with the transport process and affect the barrier integrity, as well as compromise further experiments on the tested cells [72]. The mostly used tracer is the FITC-labeled dextran with different molecular weights (4, 10, 20, 40, or 70 kDa), and the outcome of its passage through the endothelium allows a quantitative assessment of how close a hBBB-on-chip model is to the *in vivo* BBB. Indeed, Campisi and co-workers developed a 3D hBBB-on-chip model with hiPSC-derived ECs in a static tri-culture with primary brain pericytes and astrocytes, whose permeability resulted close to the recorded value *in vivo* [50]. Also, Vatine and colleagues reported a physiologically relevant permeability of their 2D hBBB-on-chip model by co-culturing hiPSC-derived ECs under continuous flow with primary brain pericytes and astrocytes [57]. In both models, despite the differences in design, hiPSC-derived ECs cultured alone showed a higher permeability than the co-cultures. However, in any culture conditions, the magnitude order of the recorded permeability coefficients was the same as the *in vivo* BBB permeability values and lower than the coefficients of other hBBB-on-chip models, even of those similar in design but without hiPSC-derived ECs [49, 52].

5.3. TEER readings

Reading *in vitro* TEER is a sensitive, non-invasive method to monitor live cells during various stages of growth, differentiation, or experimental treatment. Generally, TEER measurements are based on reading ohmic resistance or measuring impedance across a wide spectrum of frequencies. Conventional TEER electrodes are not suitable for use in OoC systems due to their microscale design. Indeed, electrodes should be integrated along the microchannels to ensure a uniform current density and an equal potential drop over the entire cell culture area. In this case, in addition to the high technical complexity, the risk of cell coverage of the electrode surfaces may compromise the measurement [72].

A hBBB-on-chip model typically requires a dedicated measurement setup and presents specific challenges for assessing the TEER values (figure 5). However, in some models, where ECs, pericytes, and astrocytes are co-cultured in a fully 3D organization, TEER measurement is unworkable because of the challenges for the electrodes integration as well as for ensuring a uniform electric field along the culture area [50–52]. Additionally, multiple factors may affect the TEER readings on a chip: temperature, physical support for cell culture, and characteristics of the electrodes such as material, quality, and surface state. Finally, other potential sources of measurement errors are chip-to-chip variation in the positioning of the electrodes and air bubbles trapped in the microchannels [71]. Therefore, a comparison among

different hBBB-on-chip models based on TEER values is not trusted yet, but TEER readings can be used to guide the internal decision-making of researchers to optimize the cell culture protocols on-chip by associating the TEER outcomes with those of the immunostaining and the permeability studies. For instance, Ahn *et al* reported a customized set-up adapted to a commercially available volt-ohmmeter (EVOM2) (figure 5(A)). They recorded TEER values from their model under different levels of shear stress and used them for the cross-validation of permeability coefficient analysis. Although recorded TEER values were lower than *in vivo*, the measurements suggested the enhancement of barrier integrity when the applied shear stress was physiologically relevant [49]. Instead, Vatine and co-workers used a specific chip design integrating electrodes for TEER readings, as previously developed by Maoz *et al* (figure 5(B)) [77]. TEER measurements on their model under high shear stress and based on hiPSC-derived ECs, co-cultured with primary pericytes and astrocytes, reached physiologically relevant values [57].

6. hBBB-on-chip models applications

Despite the variety of hBBB-on-chip models reported in the literature, there are only a few examples in which they have been demonstrated to be applied in the medical or toxicological fields. Most studies remark on the potentiality of the approach and refer to future research for specific applications. This may be attributed to the OoCs complexity itself, thus the authors are mainly focused on developing an architecture acting as a 'cell container' with well-arranged cell assembly in a way as close as possible to *in vivo* BBB for molecular permeability, TJs expression, and TEER values. However, some application cases of the hBBB-on-chip models exist and prove the superiority of these models as compared with *in vivo* animal models or other *in vitro* systems. For example, Lee *et al* have demonstrated the potentiality of their 3D hBBB-on-chip model in studying the mechanism of inhibitors of efflux transporters, in particular the p-glycoprotein, for the use in drug co-treatment and have suggested further applications to evaluate CNS medications targeting pathological angiogenesis associated with brain tumors or brain damage [52]. Some hBBB-on-chip models have been used to assess the transcytosis across the barrier of therapeutic antibodies, thus demonstrating that these *in vitro* models are able to support the discovery/engineering of novel BBB-shuttle technologies [61]. Other models have been used to study the effect of intravascular administration of methamphetamine, a psychoactive drug, and to identify previously unknown metabolic interactions between the BBB and neurons [56]. Ahn's model was exploited to evaluate lipid-nanoparticle distributions at cellular levels and to assess the distinct cellular uptakes and BBB crossing mechanisms through receptor-mediated transcytosis [49]. This allowed to demonstrate the huge potentialities of Ahn's platform to screen drug candidates for the treatment of neurological diseases. The study of distinct contributions of astrocytes and pericytes to neuroinflammation was the main target of Herland's model. Indeed, when their model was stimulated with the inflammatory trigger tumor necrosis factor-α, the authors reported different secretion profiles for granulocyte colony-stimulating factor and interleukin-6, depending on the presence of astrocytes or pericytes [53]. A model study to investigate the BBB disruption in various diseases, including acute liver failure and melanoma, was developed by Motallebnejad *et al* who showed the effects of apical delivery of the transforming growth factor β on BBB integrity and astrocyte activation as an effect of high plasma levels of the same factor [48]. Finally, it should be remembered the Vatine's model, incorporating hiPSCs-derived ECs of Huntington's disease (HD) patients, to assess the using a personalized hBBB-on-chip model as a predictor for patient-specific brain penetrability of candidate molecules [57].

7. Conclusions

Models of hBBB based on OoC technology represent a disruptive technology with several advantages, but still some weaknesses. From a technical point of view, their implementation is not straightforward and well targeted efforts are needed to develop standardized and validated models for toxicological screening and for studying various diseases in which the hBBB district is involved. Nevertheless, the works reported in the literature are consistent enough to demonstrate the potential of these OoC platforms as compared to other hBBB *in vitro* and *in vivo* animal models. Indeed, OoCs were found to be more effective in predicting human response than the traditional *in vitro* cell cultures and *in vivo* methods of animal testing and, therefore, to be efficient in preclinical predictions [78]. On the other hand, being the traditional animal models quite expensive, there is a growing need of designing innovative cost-effective hBBB models to accelerate the development of novel drugs and decrease the considerable costs of failure in preclinical predictions and clinical tests. For all these reasons, once routinely accepted in common practice, hBBB-on-chip models are expected to sensibly reduce the number of animal testing and speed up the process of novel drug testing in the pharmaceutical industry. However, to move towards standardization, more focused research is needed to establish and validate the most convenient design strategy for better mimicking the hBBB. Regarding the most convenient cell types to be included in a hBBB-on-chip model, although hiPSCs technology offers interesting perspectives for the development of personalized models,

its current immaturity and high costs are such that primary cells ensure more chance for reliability and reproducibility [69].

Then, a step forward would be to reduce fabrication costs by moving from techniques such as 3D printing, soft lithography, hot embossing, and injection molding to bioprinting, which has been considered by many researchers as a more cost-efficient fabrication process for OoCs [79]. Another important issue that could act in favor of adopting OoCs for modelling hBBB is that microfluidic technology allows easy integration of sensors into the chips, which makes monitoring key physiological parameters easier compared to traditional methods [80, 81]. Far from being considered a purly academic exercise, the development of hBBB-on-chip models is also interesting for medtech companies and emerging start-ups. Some of them (i.e. SynVivo, Emulate) already sell microfluidic devices with biological/chemical components kits required to model the hBBB that researchers can use to perform drug permeability assays, to evaluate toxicity effects of chemical, biological, and physical agents on the cells of the hBBB, to study the effect of drugs with potential protective effects on the hBBB, to investigate the effects of tumor cells and inflammatory factors on the hBBB, to visualize and quantify tight junction, transporter proteins or the migration of immune cells, and for a genomic, proteomic, and metabolic analysis of normal and dysfunctional hBBB. For instance, the effects of hyperthermia treatment with magnetic nanoparticles on glioblastoma were demonstrated by using a commercial microfluidic platform [82], but several other applications can be imaged such as testing of treatments with ultrasounds to increase BBB permeability to drugs, methods to identify personalized doses of drugs, testing of drug or stem cell-loaded nanocarriers that cross the BBB, etc.

In conclusion, hBBB-on-chip models are poised to become broadly accepted in biomedical and pharmaceutical research because of their higher biologic fidelity and lower cost compared to traditional methods, although strong cooperation with researchers and industry must be forced to develop and validate processes. These joint efforts are necessary to promote the technological improvements that can facilitate the widespread adoption of OoC-based hBBB models for preclinical and clinical studies.

8. Future perspectives

As we discussed so far in this work, the development of hBBB-on-chip models has made substantial technological advancements over the last decade, but recently there has been increasing interest in modelling various neurological diseases such as Alzheimer's disease (AD) and Parkinson's disease (PD) using such technology [83, 84]. Recent findings in AD research have established that BBB impairment is related to AD pathogenesis. Although just a few hBBB-on-chip models have been successfully applied to AD research, they showed to be more promising than traditional *in vitro* hBBB transwell models to enable the accurate quantification of beta-amyloid (Aβ) accumulation around the perivascular area and Aβ clearance from the BBB [85]. Modelling a brain disease in a hBBB-on-chip model can be also used to better predict drug responses. For instance, glioblastoma (GBM) spheroids were added in a hBBB-on-chip model to study BBB-associated chemosensitivity and drug delivery in GBM [86]. These examples of recent works allow us to envisage the future perspectives in modelling the hBBB on a chip, which will be increasingly oriented towards the study of pathological conditions by the implementation of other cell types (e.g. neurons with specific mutations, cancer-derived cells, microglia), or towards the development of personalized models by using patient-derived cells.

Data availability statement

All data that support the findings of this study are included within the article (and any supplementary files).

Acknowledgments

The authors are grateful to 'Tecnopolo per la medicina di precisione' (TecnoMed Puglia)—Regione Puglia: DGR n.2117 del 21/11/2018, CUP: B84I18000540002 and 'Tecnopolo di Nanotecnologia e Fotonica per la medicina di precisione' (TECNOMED)—FISR/MIUR-CNR: delibera CIPE n.3449 del 7-08-2017, CUP: B83B17000010001.

ORCID iDs

Vita Guarino https://orcid.org/0000-0001-6877-5169
Alessandra Zizzari https://orcid.org/0000-0002-9651-7922
Monica Bianco https://orcid.org/0000-0002-1791-7232
Giuseppe Gigli https://orcid.org/0000-0002-2583-5747
Lorenzo Moroni https://orcid.org/0000-0003-1298-6025
Valentina Arima https://orcid.org/0000-0002-3429-8365

References

[1] Russell W M S 1995 The development of the three Rs concept *Altern. Lab. Anim.* **23** 298–304
[2] Piergiovanni M, Jenet A, Batista Leite S, Cangar O, Mian L, Maurer P, Ganesh A, Whelan M and Taucer F 2021 *Organ on chip: building a roadmap towards standardisation* JRC126163 Joint Research Centre (JRC) (https://doi.org/10.2760/819439)

[3] Reardon S 2015 'Organs-on-chips' go mainstream *Nature* **523** 266
[4] Franzen N, van Harten W H, Retèl V P, Loskill P, van den Eijnden-van Raaij J and IJzerman M 2019 Impact of organ-on-a-chip technology on pharmaceutical R&D costs *Drug Discov. Today* **24** 1720–4
[5] Jiang L, Li S, Zheng J, Li Y and Huang H 2019 Recent progress in microfluidic models of the blood-brain barrier *Micromachines* **10** 375
[6] Jackson S, Meeks C, Vézina A, Robey R W, Tanner K and Gottesman M M 2019 Model systems for studying the blood-brain barrier: applications and challenges *Biomaterials* **214** 119217
[7] Perrin S 2014 Preclinical research: make mouse studies work *Nature* **507** 423–5
[8] Kuhnline Sloan C D, Nandi P, Linz T H, Aldrich J V, Audus K L and Lunte S M 2012 Analytical and biological methods for probing the blood-brain barrier *Annu. Rev. Anal. Chem.* **5** 505–31
[9] Shih A Y, Driscoll J D, Drew P J, Nishimura N, Schaffer C B and Kleinfeld D 2012 Two-photon microscopy as a tool to study blood flow and neurovascular coupling in the rodent brain *J. Cereb. Blood Flow Metab.* **32** 1277–309
[10] Stone N L, England T J and O'Sullivan S E 2019 A novel transwell blood brain barrier model using primary human cells *Front. Cell. Neurosci.* **13** 230
[11] Bhalerao A, Sivandzade F, Archie S R, Chowdhury E A, Noorani B and Cucullo L 2020 *In vitro* modeling of the neurovascular unit: advances in the field *Fluids Barriers CNS* **17** 22
[12] DeStefano J G, Xu Z S, Williams A J, Yimam N and Searson P C 2017 Effect of shear stress on iPSC-derived human brain microvascular endothelial cells (dhBMECs) *Fluids Barriers CNS* **14** 20
[13] De Luca C, Colangelo A M, Virtuoso A, Alberghina L and Papa M 2020 Neurons, glia, extracellular matrix and neurovascular unit: a systems biology approach to the complexity of synaptic plasticity in health and disease *Int. J. Mol. Sci.* **21** 1539
[14] Peyrounette M, Davit Y, Quintard M and Lorthois S 2018 Multiscale modelling of blood flow in cerebral microcirculation: Details at capillary scale control accuracy at the level of the cortex *PLoS ONE* **13** e0189474
[15] Abbott N J, Rönnbäck L and Hansson E 2006 Astrocyte–endothelial interactions at the blood–brain barrier *Nat. Rev. Neurosci.* **7** 41–53
[16] Wong A D, Ye M, Levy A F, Rothstein J D, Bergles D E and Searson P C 2013 The blood-brain barrier: an engineering perspective *Front. Neuroeng.* **6** 7
[17] Mastorakos P and McGavern D 2019 The anatomy and immunology of vasculature in the central nervous system *Sci. Immunol.* **4** eaav0492
[18] Zlokovic B V 2008 The blood-brain barrier in health and chronic neurodegenerative disorders *Neuron* **57** 178–201
[19] Kinney J P, Spacek J, Bartol T M, Bajaj C L, Harris K M and Sejnowski T J 2013 Extracellular sheets and tunnels modulate glutamate diffusion in hippocampal neuropil *J. Comp. Neurol.* **521** 448–64
[20] Ye M, Sanchez H M, Hultz M, Yang Z, Bogorad M, Wong A D and Searson P C 2015 Brain microvascular endothelial cells resist elongation due to curvature and shear stress *Sci. Rep.* **4** 4681
[21] Nag S 2003 Morphology and Molecular Properties of Cellular Components of Normal Cerebral Vessels. *The Blood-Brain Barrier* vol 89 ed Nag S Methods in Molecular Medicine (Totowa, NJ: Humana Press) pp 3–36
[22] Moya M L *et al* 2020 A reconfigurable *in vitro* model for studying the blood–brain barrier *Ann. Biomed. Eng.* **48** 780–93
[23] Shin Y, Choi S H, Kim E, Bylykbashi E, Kim J A, Chung S, Kim D Y, Kamm R D and Tanzi R E 2019 Blood–brain barrier dysfunction in a 3D *in vitro* model of Alzheimer's disease *Adv. Sci.* **6** 1900962
[24] Dore-Duffy P and Cleary K 2011 Morphology and properties of pericytes *The Blood-Brain and Other Neural Barriers* vol 686, ed S Nag Methods in Molecular Biology (Totowa, NJ: Humana Press) pp 49–68
[25] Shepro D and Morel N M L 1993 Pericyte physiology *FASEB J.* **7** 1031–8
[26] Dore-Duffy P, Owen C, Balabanov R, Murphy S, Beaumont T and Rafols J A 2000 Pericyte migration from the vascular wall in response to traumatic brain injury *Microvasc. Res.* **60** 55–69
[27] Dore-Duffy P, Katychev A, Wang X and Van Buren E 2006 CNS microvascular pericytes exhibit multipotential stem cell activity *J. Cereb. Blood Flow Metab.* **26** 613–24
[28] Peppiatt C M, Howarth C, Mobbs P and Attwell D 2006 Bidirectional control of CNS capillary diameter by pericytes *Nature* **443** 700–4
[29] Kisler K, Nikolakopoulou A M, Sweeney M D, Lazic D, Zhao Z and Zlokovic B V 2020 Acute ablation of cortical pericytes leads to rapid neurovascular uncoupling *Front. Cell. Neurosci.* **14** 27
[30] Jamieson J J, Linville R M, Ding Y Y, Gerecht S and Searson P C 2019 Role of iPSC-derived pericytes on barrier function of iPSC-derived brain microvascular endothelial cells in 2D and 3D *Fluids Barriers CNS* **16** 15
[31] Mathiisen T M, Lehre K P, Danbolt N C and Ottersen O P 2010 The perivascular astroglial sheath provides a complete covering of the brain microvessels: an electron microscopic 3D reconstruction *Glia* **58** 1094–103
[32] Iliff J J *et al* 2012 A paravascular pathway facilitates CSF flow through the brain parenchyma and the clearance of interstitial solutes, including amyloid β *Sci. Transl. Med.* **4** 147ra111
[33] Iliff J J, Lee H, Yu M, Feng T, Logan J, Nedergaard M and Benveniste H 2013 Brain-wide pathway for waste clearance captured by contrast-enhanced MRI *J. Clin. Invest.* **123** 1299–309
[34] Michinaga S and Koyama Y 2019 Dual roles of astrocyte-derived factors in regulation of blood-brain barrier function after brain damage *Int. J. Mol. Sci.* **20** 571
[35] Dudvarski Stankovic N, Teodorczyk M, Ploen R, Zipp F and Schmidt M H H 2016 Microglia-blood vessel interactions: a double-edged sword in brain pathologies *Acta Neuropathol.* **131** 347–63
[36] Mondo E, Becker S C, Kautzman A G, Schifferer M, Baer C E, Chen J, Huang E J, Simons M and Schafer D P 2020 A developmental analysis of juxtavascular microglia dynamics and interactions with the vasculature *J. Neurosci.* **40** 6503–21
[37] Ronaldson P T and Davis T P 2020 Regulation of blood–brain barrier integrity by microglia in health and disease: a therapeutic opportunity *J. Cereb. Blood Flow Metab.* **40** S6–24
[38] Thurgur H and Pinteaux E 2019 Microglia in the neurovascular unit: blood–brain barrier–microglia interactions after central nervous system disorders *Neuroscience* **405** 55–67
[39] Zimmermann D R and Dours-Zimmermann M T 2008 Extracellular matrix of the central nervous system: from neglect to challenge *Histochem. Cell Biol.* **130** 635–53
[40] Xu L, Nirwane A and Yao Y 2019 Basement membrane and blood–brain barrier *Stroke Vasc. Neurol.* **4** 78–82
[41] Ulbrich P, Khoshneviszadeh M, Jandke S, Schreiber S and Dityatev A 2021 Interplay between perivascular and perineuronal extracellular matrix remodelling in neurological and psychiatric diseases *Eur. J. Neurosci.* **53** 3811–30
[42] Cui B and Cho S-W 2022 Blood-brain barrier-on-a-chip for brain disease modeling and drug testing *BMB Rep.* **55** 213–9

[43] Wang Y I, Abaci H E and Shuler M L 2017 Microfluidic blood–brain barrier model provides in vivo-like barrier properties for drug permeability screening *Biotechnol. Bioeng.* **114** 184–94
[44] Marino A, Tricinci O, Battaglini M, Filippeschi C, Mattoli V, Sinibaldi E and Ciofani G 2018 A 3D real-scale, biomimetic, and biohybrid model of the blood-brain barrier fabricated through two-photon lithography *Small* **14** 1702959
[45] Miri A K, Mostafavi E, Khorsandi D, Hu S-K, Malpica M and Khademhosseini A 2019 Bioprinters for organs-on-chips *Biofabrication* **11** 042002
[46] Kolesky D B, Homan K A, Skylar-Scott M A and Lewis J A 2016 Three-dimensional bioprinting of thick vascularized tissues *Proc. Natl Acad. Sci.* **113** 3179–84
[47] Dobos A, Gantner F, Markovic M, Van Hoorick J, Tytgat L, Van Vlierberghe S and Ovsianikov A 2021 On-chip high-definition bioprinting of microvascular structures *Biofabrication* **13** 015016
[48] Brown J A *et al* 2015 Recreating blood-brain barrier physiology and structure on chip: a novel neurovascular microfluidic bioreactor *Biomicrofluidics* **9** 054124
[49] Motallebnejad P, Thomas A, Swisher S L and Azarin S M 2019 An isogenic hiPSC-derived BBB-on-a-chip *Biomicrofluidics* **13** 064119
[50] Ahn S I, Sei Y J, Park H-J, Kim J, Ryu Y, Choi J J, Sung H-J, MacDonald T J, Levey A I and Kim Y 2020 Microengineered human blood–brain barrier platform for understanding nanoparticle transport mechanisms *Nat. Commun.* **11** 175
[51] Campisi M, Shin Y, Osaki T, Hajal C, Chiono V and Kamm R D 2018 3D self-organized microvascular model of the human blood-brain barrier with endothelial cells, pericytes and astrocytes *Biomaterials* **180** 117–29
[52] Osaki T, Sivathanu V and Kamm R D 2018 Engineered 3D vascular and neuronal networks in a microfluidic platform *Sci. Rep.* **8** 5168
[53] Lee S, Chung M, Lee S-R and Jeon N L 2020 3D brain angiogenesis model to reconstitute functional human blood–brain barrier *in vitro Biotechnol. Bioeng.* **117** 748–62
[54] Herland A, van der Meer A D, FitzGerald E A, Park T-E, Sleeboom J J F and Ingber D E 2016 Distinct contributions of astrocytes and pericytes to neuroinflammation identified in a 3D human blood-brain barrier on a chip *PLoS One* **11** e0150360
[55] Partyka P P, Godsey G A, Galie J R, Kosciuk M C, Acharya N K, Nagele R G and Galie P A 2017 Mechanical stress regulates transport in a compliant 3D model of the blood-brain barrier *Biomaterials* **115** 30–39
[56] Pereira R F and Bártolo P J 2015 3D bioprinting of photocrosslinkable hydrogel constructs *J. Appl. Polym. Sci.* **132** 42458
[57] Maoz B M *et al* 2018 A linked organ-on-chip model of the human neurovascular unit reveals the metabolic coupling of endothelial and neuronal cells *Nat. Biotechnol.* **36** 865–74
[58] Vatine G D *et al* 2019 Human iPSC-derived blood-brain barrier chips enable disease modeling and personalized medicine applications *Cell Stem. Cell* **24** 995–1005.e6
[59] Zakharova M, Do Carmo M A P, van der Helm M W, Le-The H, de Graaf M N S, Orlova V, van den Berg A, van der Meer A D, Broersen K and Segerink L I 2020 Multiplexed blood–brain barrier organ-on-chip *Lab. Chip* **20** 3132–43
[60] Tibbe M P, Leferink A M, van den Berg A, Eijkel J C T and Segerink L I 2018 Microfluidic gel patterning method by use of a temporary membrane for organ-on-chip applications *Adv. Mater. Technol.* **3** 1700200
[61] Nguyen T P T, Tran B M and Lee N Y 2018 Microfluidic approach for the fabrication of cell-laden hollow fibers for endothelial barrier research *J. Mater. Chem.* B **6** 6057–66
[62] Wevers N R *et al* 2018 A perfused human blood–brain barrier on-a-chip for high-throughput assessment of barrier function and antibody transport *Fluids Barriers CNS* **15** 23
[63] Brown T D, Nowak M, Bayles A V, Prabhakarpandian B, Karande P, Lahann J, Helgeson M E and Mitragotri S 2019 A microfluidic model of human brain (μHuB) for assessment of blood brain barrier *Bioeng. Transl. Med.* **4** e10126
[64] Aran K, Sasso L A, Kamdar N and Zahn J D 2010 Irreversible, direct bonding of nanoporous polymer membranes to PDMS or glass microdevices *Lab. Chip* **10** 548
[65] Arık Y B, de Sa Vivas A, Laarveld D, van Laar N, Gemser J, Visscher T, van den Berg A, Passier R and van der Meer A D 2021 Collagen I based enzymatically degradable membranes for organ-on-a-chip barrier models *ACS Biomater. Sci. Eng.* **7** 2998–3005
[66] Huang B, He Y, Wang L, Shi J, Hu J, Rofaani E, Yamada A and Chen Y 2020 Microfluidic channel with embedded monolayer nanofibers for cell culture and co-culture *Microelectron. Eng.* **225** 111235
[67] Qi D *et al* 2018 Establishment of a human iPSC- and nanofiber-based microphysiological blood–brain barrier system *ACS Appl. Mater. Interfaces* **10** 21825–35
[68] Bernas M J *et al* 2010 Establishment of primary cultures of human brain microvascular endothelial cells to provide an *in vitro* cellular model of the blood-brain barrier *Nat. Protocols* **5** 1265–72
[69] Weksler B B *et al* 2005 Blood-brain barrier-specific properties of a human adult brain endothelial cell line *FASEB J.* **19** 1872–4
[70] Logan S, Arzua T, Canfield S G, Seminary E R, Sison S L, Ebert A D and Bai X 2019 Studying human neurological disorders using induced pluripotent stem cells: from 2D monolayer to 3D organoid and blood brain barrier models *Compr. Physiol.* **9** 565–611
[71] Caliari S R and Burdick J A 2016 A practical guide to hydrogels for cell culture *Nat. Methods* **13** 405–14
[72] Arık Y B, van der Helm M W, Odijk M, Segerink L I, Passier R, van den Berg A and van der Meer A D 2018 Barriers-on-chips: measurement of barrier function of tissues in organs-on-chips *Biomicrofluidics* **12** 042218
[73] Srinivasan B, Kolli A R, Esch M B, Abaci H E, Shuler M L and Hickman J J 2015 TEER measurement techniques for *in vitro* barrier model systems *SLAS Technol.* **20** 107–26
[74] Shi L, Zeng M, Sun Y and Fu B M 2014 Quantification of blood-brain barrier solute permeability and brain transport by multiphoton microscopy *J. Biomech. Eng.* **136** 031005
[75] Butt A M, Jones H C and Abbott N J 1990 Electrical resistance across the blood-brain barrier in anaesthetized rats: a developmental study *J. Physiol.* **429** 47–62
[76] Butt A M and Jones H C 1992 Effect of histamine and antagonists on electrical resistance across the blood-brain barrier in rat brain-surface microvessels *Brain Res.* **569** 100–5
[77] Smith Q R and Rapoport S I 1986 Cerebrovascular permeability coefficients to sodium, potassium, and chloride *J. Neurochem.* **46** 1732–42
[78] Maoz B M *et al* 2017 Organs-on-Chips with combined multi-electrode array and transepithelial electrical resistance measurement capabilities *Lab. Chip* **17** 2294–302
[79] Leung C M *et al* 2022 A guide to the organ-on-a-chip *Nat. Rev. Methods Primer* **2** 1–29
[80] Carvalho V, Gonçalves I, Lage T, Rodrigues R O, Minas G, Teixeira S F C F, Moita A S, Hori T, Kaji H and Lima R A 2021 3D printing techniques and their applications to organ-on-a-chip platforms: a systematic review *Sensors* **21** 3304
[81] Clarke G A *et al* 2021 Advancement of sensor integrated organ-on-chip devices *Sensors* **21** 1367
[82] Rothbauer M, Bachmann B E M, Eilenberger C, Kratz S R A, Spitz S, Höll G and Ertl P 2021 A decade of organs-on-a-chip emulating human physiology at the microscale: a critical status report on progress in toxicology and pharmacology *Micromachines* **12** 470

[83] Mamani J B, Marinho B S, Rego G N D A, Nucci M P, Alvieri F, Santos R S D, Ferreira J V M, Oliveira F A D and Gamarra L F 2019 Magnetic hyperthermia therapy in glioblastoma tumor on-a-Chip model *Einstein São Paulo* **18** eAO4954

[84] Pediaditakis I *et al* 2021 Modeling alpha-synuclein pathology in a human brain-chip to assess blood-brain barrier disruption *Nat. Commun.* **12** 5907

[85] Yoon J, Kim J, Shah Z, Awasthi A, Mahajan A and Kim Y 2021 Advanced human BBB-on-a-chip: a new platform for Alzheimer's disease studies *Adv. Healthcare Mater.* **10** 2002285

[86] Seo S, Nah S, Lee K, Choi N and Kim H N 2022 Triculture model of *in vitro* BBB and its application to study BBB-associated chemosensitivity and drug delivery in glioblastoma *Adv. Funct. Mater.* **32** 2106860